

Potential-Energy Landscapes of Simple Liquids

Pooja Shah and Charusita Chakravarty*

Department of Chemistry, Indian Institute of Technology–Delhi, Hauz Khas, New Delhi: 110016, India
(Received 7 December 2001; published 5 June 2002)

Changes in the potential-energy surface as a function of the range and curvature of the pair potential are studied using isothermal-isobaric ensemble Monte Carlo simulations of Morse liquids. The configurational energies of stationary points are found to be linear functions of the fraction of imaginary modes, with slopes that are proportional to the range of the potential. The relative energies of saddles, minima, and instantaneous configurations show qualitatively different behavior for short, long, and intermediate range potentials, which imply corresponding variations in liquid state relaxation dynamics.

DOI: 10.1103/PhysRevLett.88.255501

PACS numbers: 61.20.Lc

The potential-energy surface, U , of an interacting collection of atoms is a scalar function of the $3N$ -dimensional position vector, \mathbf{r} , and contains, in principle, all the information necessary to understand the collective properties. The inherent structure approach concentrates on the properties of local minima of $U(\mathbf{r})$ and has provided a very useful descriptive tool for understanding melting and the glass transition [1–9]. Recent work has focused on the properties of stationary points or inherent saddles of the potential energy surface (PES), which correspond to absolute minima of the pseudopotential surface, $W(\mathbf{r}) = \frac{1}{2}|\nabla U|^2$, in order to understand the glass transition [10–15]. Model glass formers, such as the binary Lennard-Jones mixture, the binary soft-sphere mixture, and the modified Lennard-Jones (MLJ) liquid, have been shown to undergo a transition from saddle-dominated to minima-dominated dynamical regimes at the mode-coupling transition temperature, T_{MC} . Saddles are stationary points of order 1 or more and mark the border between adjoining basins of two minima. For $T > T_{MC}$, the system is localized largely in border regions and basin hopping is facile. Below T_{MC} , the system occupies interiors of the basins of local minima, and basin hopping becomes an activated process. A computational problem arises in the mapping of absolute minima of the pseudopotential, $W(\mathbf{r})$, to the stationary points of the true potential $U(\mathbf{r})$ because any minimization algorithm will also tend to sample low-lying minima of $W(\mathbf{r})$ which correspond to inflection points of $U(\mathbf{r})$, rather than true saddles [16]. Careful numerical investigation of this issue, however, shows that the number of inflection directions is always very small and does not significantly affect the statistical estimates of saddle properties [14,15,17,18]. Therefore these low-lying minima of $W(\mathbf{r})$ may be designated as quasisaddles (abbreviated to saddles in this work) and may be regarded as constituting a dynamically significant set of points on the PES which show a qualitative change in properties near the mode-coupling transition temperature [10,16].

Since a glass may be viewed as a very high-viscosity liquid, it is expected that many of the statistical features of the stationary points of the PES of glass formers will be shared by simple liquids, as shown recently in the case

of the Lennard-Jones (LJ) liquid [19]. The present study explores the physical significance of the inherent saddles by studying the correlation between their statistical properties and generic features of the interatomic potential for simple liquids. In particular, we study liquids bound by Morse pair potentials

$$V_{\alpha}(r) = \epsilon[e^{-\alpha[1-(r/r_e)]} - 1]^2 - \epsilon \quad (1)$$

sharing a common well depth, ϵ , and equilibrium pair distance, r_e , but with different values of the range parameter, α , which is inversely correlated with the range and softness of the potential. We show that changes in the saddle properties with α reflect the changing topography of the PES and provide insights into how the system dynamics is likely to change as the pair potential changes in curvature and range. These results should be fairly general, since the Morse potentials can be used to fit bulk and diatomic data for a wide range of systems, e.g., metallic systems have $\alpha \approx 3$, rare gases have $\alpha \approx 6$, while a very short-range system such as C_{60} has $\alpha = 13.7$ [20]. Since this work focuses on the liquid state, rather than the glassy regime, it is not necessary to include a many-body potential term to inhibit crystallization.

Isothermal-isobaric ensemble Monte Carlo simulations of Morse liquids with $4 \leq \alpha \leq 12$ are performed at temperatures, T , between 0.675 and 1.5 and pressure $P = 0.933$ [21–23]. A rhombic dodecahedral simulation cell with 125 particles was used. Spherical potential cut-off distances of $\approx 2.5r_e$ and long-range corrections were employed. The 100 instantaneous configurations were sampled from runs of length 5×10^6 . Starting with an instantaneous configuration, local minimizations on the $U(\mathbf{r})$ and $W(\mathbf{r})$ surfaces were used to generate the corresponding inherent minimum and saddle, respectively, keeping volume constant during the minimization. A limited memory quasi-Newton method for multidimensional optimization, referred to as the LBFGS algorithm, was used for the local minimizations [24]. Finite potential cutoffs imply that minimization with maximum precision will be difficult and a high proportion of low-lying minima of $W(\mathbf{r})$ may be sampled [25]. Based on the recent work on this issue [14–19], a convergence criteria of 10^{-9} for

the LBFGS algorithm should be sufficient to converge the ensemble averaged saddle energies to 1%. For convenience, we refer to all minima of $W(\mathbf{r})$ sampled within the precision limits of the LBFGS algorithm as saddles.

A saddle point is characterized by its configurational energy, U_s , and its index density, n_s , which corresponds to the fraction of imaginary modes; the NPT averages are denoted by $\langle U \rangle_s$ and $\langle n \rangle_s$. Previous studies have shown that the points $(\langle U \rangle_s, \langle n \rangle_s)$, with T treated as a parameter, lie on a straight line of slope $\partial U_s / \partial n_s$ and intercept U_{thr} [26]. Figure 1 confirms this linear relationship for all the Morse systems examined here. However, as shown in Table I, the slopes, $\partial U_s / \partial n_s$, decrease and the intercepts, U_{thr} , increase with increasing α . The threshold energy, U_{thr} , marks the border between saddle- and minima-dominated portions of the energy landscape. The lowering of U_{thr} as the range increases is due to the increase in binding energies of Morse liquids with increasing range [23].

The linear form of the $\langle U \rangle_s(\langle n \rangle_s)$ curves and the variation in $\partial U_s / \partial n_s$ with α can be understood on the basis of a localized mechanism for generating imaginary frequency displacement modes which requires rearrangement of only a few neighboring atoms. The slope $\partial U_s / \partial n_s$ will depend on the change in U due to such a local disturbance. The shorter the range of the potential, the fewer the number of neighbors that will feel the perturbation, the smaller the spatial range of influence of the perturbation, and the smaller the slope of the $\langle U \rangle_s(\langle n \rangle_s)$ line. Earlier studies have identified β processes in supercooled liquids with relaxations between neighboring basins involving localized particle rearrangements [1,2]. The barrier heights associated with β processes must correspond to $(\partial U_s / \partial n_s)$. In the solid phase with high packing densities, the defect generation mechanism is unlikely to be localized. Therefore, this linear dependence of saddle energies on index densities is likely to be a general characteristic of liquids. Our results extend the earlier work on minima and transition

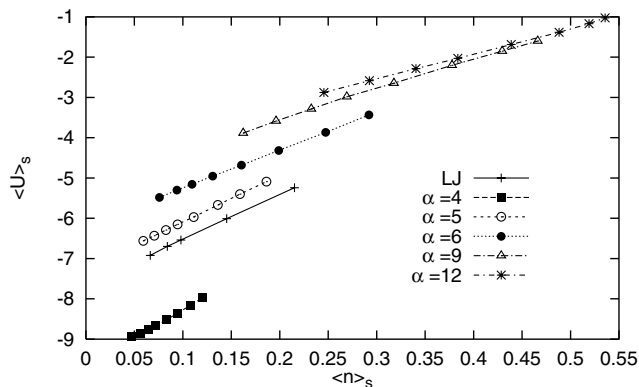


FIG. 1. Plot of the average configurational energy of saddles, $\langle U \rangle_s(T)$, against the average index density, $\langle n \rangle_s(T)$. Results for Morse potentials with different values of α are compared with those for the Lennard-Jones (LJ) liquid. $\langle U \rangle_s$ is given in units of ϵ per atom.

states of finite Morse clusters which also indicated a general flattening of the PES with increasing α [3,4].

We next compare the temperature dependence of the average saddle index densities, $\langle n \rangle_s$, to the corresponding instantaneous quantity $\langle n \rangle_i$, for different Morse liquids. While instantaneous normal mode approaches have shown that $\langle n \rangle_i$ is strongly correlated with the diffusivity, a rigorous relation between the two is difficult to obtain because $\langle n \rangle_i$ normally includes a substantial contribution from non-diffusive shoulder modes [27–31]. It has been suggested that minimization on the $W(\mathbf{r})$ surface may remove most of the nondiffusive modes and, therefore, $\langle n \rangle_s$ may prove to be better correlated with the diffusivity [10,19]. In the context of the glass transition, it has been shown that $n_s(T)$ goes to zero close to T_{MC} .

Figure 2 compares $\langle n \rangle_s$ and $\langle n \rangle_i$ for liquids with $\alpha = 4, 6, \text{ and } 12$. For all values of α and T , $\langle n \rangle_s$ is less than $\langle n \rangle_i$; however, as T or α increases, $\langle n \rangle_s$ approaches $\langle n \rangle_i$. At a given temperature, $\langle n \rangle_s$ increases with decreasing range of the pair potential. We fitted the data for $\langle n \rangle_s$ to a functional form $A(T - T_{\text{MC}})^\gamma$ (see Table I). The γ values are maximum for the intermediate range Morse ($\alpha = 5$ and 6) and LJ systems.

Figure 3 compares the thermally averaged instantaneous, saddle, and inherent minima configurational energies (denoted by $\langle U \rangle_i$, $\langle U \rangle_s$, and $\langle U \rangle_m$, respectively) for the $\alpha = 4$ and 12 Morse liquids. At a given temperature, the saddle configurational energies for the $\alpha = 4$ system are closer to those of minima rather than instantaneous configurations. As α increases, $\langle U \rangle_s$ moves closer to $\langle U \rangle_i$, and Fig. 3(b) shows the corresponding curves for the very short-range V_{12} Morse liquid. Since increasing temperature tends to attenuate the effect of the attractive interactions, the difference between $\langle U \rangle_i$ and $\langle U \rangle_s$ decreases with temperature for a given value of α .

To clarify this variation in the energies of saddles relative to those of minima and instantaneous configurations, Fig. 4 plots $r(T) = [\langle U \rangle_i - \langle U \rangle_s] / [\langle U \rangle_s - \langle U \rangle_m]$ for the LJ as well as for several Morse systems. The ratio $r \approx 2$ for the longest range $\alpha = 4$ system and is ≈ 0 for the shortest range systems. For a given value of α , r decreases

TABLE I. Fitting parameters for data shown in Figs. 1 and 2. The $(\langle U \rangle_s, \langle n \rangle_s)$ data points in Fig. 2 were fitted to lines of slope $\partial U_s / \partial n_s$ and intercept U_{thr} . The $\langle n \rangle_s(T)$ data shown in Fig. 2 were fitted to the form $A(T - T_{\text{MC}})^\gamma$ by a nonlinear fitting program over the range $0.6 \leq T \leq 1.3$; the % error in the γ value is shown in the table [32].

System	$\partial U_s / \partial n_s$	U_{thr}	A	T_{MC}	γ	% error
LJ	11.2	-7.7	0.24	0.37	1.33	2.7
$\alpha = 4$	13.4	-9.6	0.14	0.48	0.64	4.9
$\alpha = 5$	11.6	-7.2	0.20	0.37	1.12	4.5
$\alpha = 6$	9.4	-6.2	0.29	0.30	1.37	4.9
$\alpha = 9$	7.5	-5.0	0.56	0.54	0.62	5.0
$\alpha = 12$	6.3	-4.4	0.62	0.61	0.34	9.0

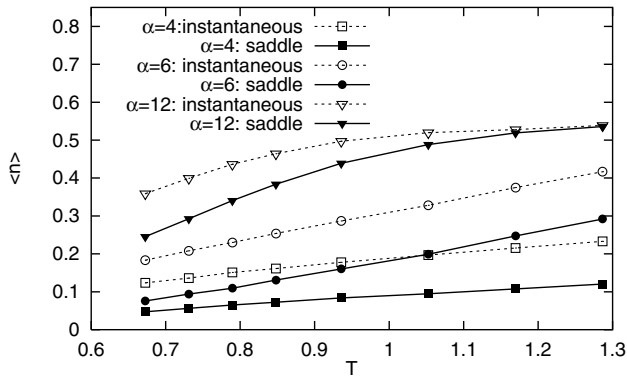


FIG. 2. Temperature dependence of the average index densities of saddle and instantaneous configurations, $\langle n \rangle_s(T)$ and $\langle n \rangle_i(T)$, respectively, for three Morse liquids.

with temperature. This is striking for the LJ, V_5 , and V_6 systems which show a transition from a high r to a low r regime. Interestingly, these are also the systems with relatively large values of γ , as shown in Table I. The large α systems must resemble binary soft-sphere mixtures which are known to be fragile glass formers [15]. Our results suggest that, as the attractive range of the potential increases, supercooled liquids should show significant variations in fragility.

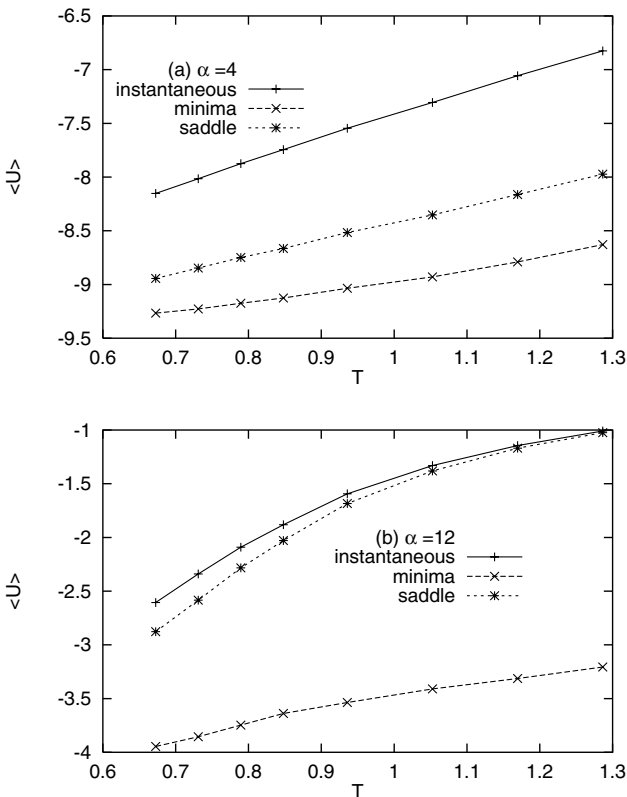


FIG. 3. Temperature-averaged configurational energies of instantaneous, inherent minima, and inherent saddles of (a) $\alpha = 4$ and (b) $\alpha = 12$ Morse systems.

The temperature dependence of $\langle n \rangle_s$, $\langle n \rangle_i$, $\langle U \rangle_s$, $\langle U \rangle_i$, and $r(T)$ indicates that resemblance between saddle and instantaneous configurations grows with T and α . The shorter the range of attraction or higher the temperature, the easier it is for an instantaneous configuration to find a nearby saddle which must imply that the density of saddle points becomes more similar to that of instantaneous configurations as $n_s(T)$ increases. Increasing T and α also results in an increase in $\langle n \rangle_s$ and $\langle n \rangle_i$. Since the number of instantaneous points must be much larger than the number of saddle points on the PES in any given energy interval, therefore the fact that $\langle n \rangle_s$ and $\langle U \rangle_s$ approach $\langle n \rangle_i$ and $\langle U \rangle_i$ as $\langle n \rangle_s$ increases must imply that the number of saddle points of order i per unit energy interval must increase with i . Studies on finite clusters do show that the number of saddle points of order i increases with i [16]. For the intermediate range Morse and LJ systems, there seems to be a shift in the density of states function which is reflected in a sharp fall in the $r(T)$ value with temperature.

Our analysis of stationary points of Morse liquids leads to the following conclusions regarding the effect of varying range and curvature of interatomic interactions on the PES landscape. In the liquid phase, the configurational energy, U_s , should depend linearly on the index density, n_s , of saddles with a slope that is proportional to the range of the potential and characterizes the overall downhill gradient associated with the metastable, amorphous packing regions of the potential energy surface. The $\langle n \rangle_s(T)$ curves are approximately fitted by a functional form $A(T - T_{MC})^\gamma$; in the temperature range studied the γ values are maximum for intermediate range potentials. The relative values of ensemble-averaged energies of saddle, minima, and instantaneous configurations are shown to have qualitatively different temperature-dependent behavior for short, intermediate, and long-range Morse systems. One may therefore expect qualitative differences in the fragility and relaxation dynamics of liquids with short, intermediate, and long-range interactions. A comparison of thermally averaged instantaneous and saddle energies and index densities leads to the conjecture that the number of stationary

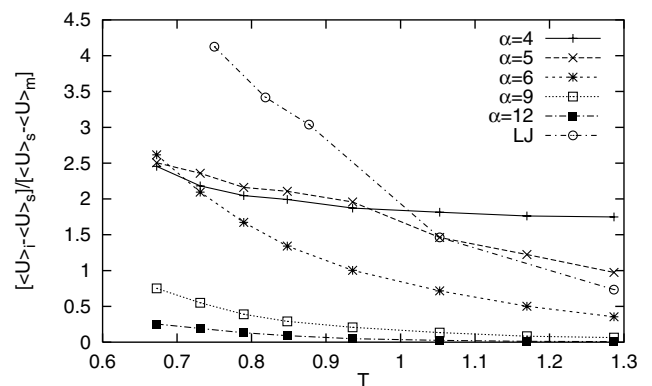


FIG. 4. The ratio $r(T) = [\langle U \rangle_i - \langle U \rangle_s] / [\langle U \rangle_s - \langle U \rangle_m]$ as a function of reduced temperature for LJ and Morse potentials.

points, for a given system size, increases with increasing index density of saddles. Our work suggests that variable range Morse systems may be convenient for studying relaxation dynamics, fragility, and aging of glasses as functions of the topographic characteristics of the potential-energy surface.

We thank R. Ramaswamy and F. Sciortino for comments and D. J. Wales for drawing our attention to Refs. [14,16]. Financial support was provided by the Council for Scientific and Industrial Research [Grant No. 01(1636)/EMR-II].

*Corresponding author.

Email address: charu@cse.iitd.ac.in

- [1] F. H. Stillinger and T. A. Weber, Phys. Rev. A **25**, 978 (1982); Science **225**, 983 (1984); J. Chem. Phys. **81**, 5095 (1984).
- [2] F. H. Stillinger, Science **267**, 1935 (1995).
- [3] J. P. K. Doye and D. J. Wales, Science **271**, 484 (1996).
- [4] D. J. Wales, J. P. K. Doye, M. A. Miller, P. N. Mortenson, and T. R. Walsh, Adv. Chem. Phys. **115**, 1 (2000).
- [5] C. A. Angell, Science **267**, 1924 (1995).
- [6] L. Angelani, G. Parisi, G. Ruocco, and G. Vilianni, Phys. Rev. Lett. **81**, 4648 (1998).
- [7] S. Sastry, Nature (London) **409**, 164 (2001).
- [8] L.-M. Martinez and C. A. Angell, Nature (London) **410**, 663 (2001).
- [9] A. Scala, F. W. Starr, E. L. Nave, F. Sciortino, and H. E. Stanley, Nature (London) **496**, 166 (2000).
- [10] L. Angelani, R. Di Leonardo, G. Ruocco, A. Scala, and F. Sciortino, Phys. Rev. Lett. **85**, 5356 (2000).
- [11] K. Broderix, K. K. Bhattacharya, A. Cavagna, A. Zippelius, and I. Giardina, Phys. Rev. Lett. **85**, 5360 (2000).
- [12] L. Angelani, R. Di Leonardo, G. Parisi, and G. Ruocco, Phys. Rev. Lett. **87**, 055502 (2001).
- [13] A. Scala, L. Angelani, R. Di Leonardo, G. Ruocco, and F. Sciortino, cond-mat/0106065.
- [14] L. Angelani, R. Di Leonardo, G. Ruocco, A. Scala, and F. Sciortino, J. Chem. Phys. (to be published).
- [15] T. S. Grigera, A. Cavagna, I. Giardina, and G. Parisi, Phys. Rev. Lett. **88**, 055502 (2002).
- [16] J. P. K. Doye and D. J. Wales, cond-mat/0108310.
- [17] P. Shah and C. Chakravarty, cond-mat/0204540.
- [18] For the 256 atom MLJ system studied in Ref. [14], no point with more than four inflection directions was found. In the liquid regime, the ratio of inflection directions to negative curvature directions was approximately 0.1. It rises to 0.8 very close to T_{MC} , but even then no major shift in the estimated value of T_{MC} was seen.
- [19] P. Shah and C. Chakravarty, J. Chem. Phys. **115**, 8784 (2001).
- [20] D. J. Wales, L. J. Munro, and J. P. K. Doye, J. Chem. Soc. Dalton Trans. **1996**, 611 (1996).
- [21] D. Frenkel and B. Smit, *Understanding Molecular Simulation: From Algorithms to Applications* (Academic Press, Boston, 1996).
- [22] All quantities are reported in reduced units with ϵ and r_e as the units of energy and length, respectively. The LJ system with the same ϵ and r_e parameters melts at $T = 0.75$ at $P = 0.933$.
- [23] P. Shah, P. Chakrabarti, and C. Chakravarty, Mol. Phys. **99**, 573 (2001).
- [24] D. C. Liu and J. Nocedal, Math. Program. **45**, 503 (1989).
- [25] Despite the reduced precision in minimization, spherical cutoffs have been used because truncating and shifting the Morse potentials removes the long-range correction terms which are crucial in determining the equilibrium densities. Moreover, the attractive simplicity of the family of Morse potentials used here which differ only in the range parameter is lost in the shifted potentials.
- [26] In the work of Broderix *et al.*, $\langle U \rangle_s$ and $\langle n \rangle_s$ are referred to as parametric averages. The average configurational energy of all saddles of index density n is referred to as the geometric average, $U_s(n_s)$. For all systems studied to date, the straight line fits to the geometric and parametric averages are identical, within the limits of statistical error.
- [27] R. M. Stratt and M. Marconelli, J. Phys. Chem. **100**, 12 981 (1996).
- [28] R. M. Stratt, Acc. Chem. Res. **28**, 201 (1995).
- [29] T. Keyes, J. Phys. Chem. **101**, 2921 (1997).
- [30] C. Donati, F. Sciortino, and P. Tartaglia, Phys. Rev. Lett. **85**, 1464 (2000).
- [31] J. D. Gezelter, E. Rabani, and B. J. Berne, J. Chem. Phys. **107**, 4618 (1997).
- [32] The parameter values have a small dependence on the temperature range over which the fit was performed. T_{MC} values are therefore not reported here since this requires simulations of substantially supercooled states which are not readily attainable in the absence of a many-body term to inhibit crystallization.